

Modelling and simulation of a fault-tolerant electrical motor for aerospace servovalves with Modelica

Gianpietro Di Rito Roberto Galatolo
Dipartimento di Ingegneria Aerospaziale - Università di Pisa (Italy)
Via Caruso, 8 – 56122 Pisa (Italy)
g.dirito@ing.unipi.it r.galatolo@ing.unipi.it

Abstract

The paper deals with the design and the simulation of electro-magnetic actuators via object-oriented modelling. The study is carried out in the Modelica-Dymola environment, and focuses on the quadruple-coil direct-drive motor of a modern fly-by-wire servovalve. Starting from basic information about material properties and from a schematic representation of the system geometry, the motor model is created mainly using the components of the *Modelica_Magnetic* library. The motor performances are then characterised with reference to both the normal operating condition (four active coils) and the worst-case fault-tolerant condition (only two active coils), in terms of current-to-force and current-to-displacement curves. The Modelica model is finally validated by comparing the simulation results with experimental data obtained during previous research activities. The Modelica results are also compared with those provided by a Matlab-Simulink model of the motor, pointing out the advantages of the object-oriented approach for the study of complex electro-magnetic systems. The easy modelling of magnetic circuit networks and the inherent simulation of magnetic material properties allow to achieve accurate results very efficiently, taking into account physical phenomena that are often disregarded during preliminary design phases, such as magnetic saturation or magnetic flux dispersions.

Keywords: fault-tolerant aircraft systems; electro-magnetic actuators; object-oriented modelling.

1 Introduction

The use of direct-drive servovalves, essentially based on the use of a rare-earth magnet electrical motor for controlling the valve spool motion,

demonstrated to be strategic for the enhancement of the performance and the reliability of modern fly-by-wire hydraulic actuators [1]. Actually, as a result of the separation between the electrical and the hydraulic section of the servovalve, fault-tolerant actuators can be obtained with simpler architectures, and the valve spool position control can be designed with great flexibility [2].

A fly-by-wire actuator with direct-drive servovalve is a complex multi-physical system, where electrical, magnetic, electronic, hydraulic and mechanical phenomena are strongly connected with each other, so the modelling and simulation can be problematic if the designer/analyst does not have technical expertise in all domains. At the same time, an actuator model is required to be accurate in the early phases of a project, well before the item is actually constructed, especially if safety-critical and high-performance application is concerned (e.g. primary flight control actuators). In this context, the object-oriented approach provided by Modelica [3, 4] can represent a very convenient solution for the rapid prototyping, the analysis, and the performance characterisation of such systems.

In the work, the model of a quadruple-coil direct-drive motor for fly-by-wire servovalves is developed in the Modelica-Dymola environment, and validated with experimental data in terms of static performances. The paper is organised into three sections. The first one reports a brief description of the system principle of work, together with a simple analytical model of the electro-magnetic section of the motor. The second part is focused on the main features of the Modelica model, mostly developed by using the components of the *Modelica_Magnetic* library [5], while the third section is dedicated to the model validation. In particular, the Modelica results are compared with both experimental data (obtained during previous research activities) and simulation

results of a Matlab-Simulink model of the motor [6], in order to point the advantages of the object-oriented modelling for the study of complex electro-magnetic systems.

2 System description

2.1 Motor layout

The internal architecture of the direct-drive motor is schematically depicted in Fig. 1. The valve spool movement is obtained by a rare-earth magnet electrical motor with four coils operating in a flux-summed configuration. When no current circulates in the coils, the armature (rigidly linked to the valve spool) is centred with respect to its endstrokes, as in this condition the centring spring is unloaded and the magnetic fluxes induced by the permanent magnets provide equal and opposite forces. When the currents are not zero, the magnetic flux induced by the coils causes an unbalanced armature polarisation. A magnetic force is therefore generated, and the resulting spool movement allows to control the actuator hydraulic power.

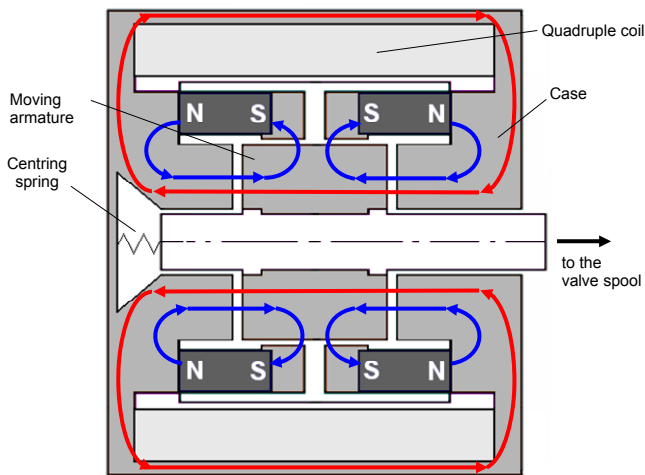


Figure 1 – Motor layout and basic magnetic network.

Modelling the dynamics of a direct-drive motor is a complex topic, since several nonlinear phenomena are involved. First of all, the magnetic force is a nonlinear function of both the current and the spool position, since the polarisation efficiency is considerably increased if the armature approaches the endstroke. Moreover, the effect of unavoidable system nonlinearities such as magnetic saturation or sliding friction cannot

be neglected if the simulation is referred to the complete range of operating conditions.

2.2 Principle of work

In order to clarify the basic working principle of the motor, a simple analytical model of the electro-magnetic section of the system is here provided. The magnetic field of the motor can be basically represented by three magnetic fluxes [7]: the one that links the coils with the variable air gaps (φ_c), and the two ones linking the left and right magnets with the left and right variable air gaps respectively (φ_{ml} and φ_{mr}).

The resulting magnetic circuit network is shown in Fig. 2.

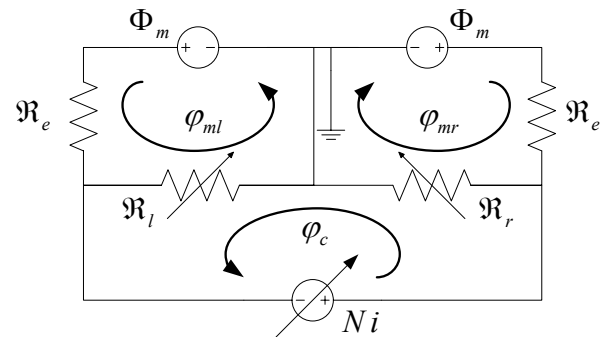


Figure 2 – Simplified magnetic network of the motor.

The network is characterised by three reluctances: two ones related to the variable air gaps (\mathfrak{R}_l and \mathfrak{R}_r), and an overall equivalent reluctance that takes into account all the soft ferrite parts, the radial clearance, and the reluctance of the permanent magnets (\mathfrak{R}_e).

Assuming that all magnetic flux tubes have the same cross-section area (A), the three reluctances are given by Eqs. (1-3), where μ is the air magnetic permeability, g is the motor air gap, and x is the armature displacement from the centred position.

$$\mathfrak{R}_e = l_e / \mu A \quad (1)$$

$$\mathfrak{R}_l = (g - x) / \mu A \quad (2)$$

$$\mathfrak{R}_r = (g + x) / \mu A \quad (3)$$

By solving the circuit equations (Eq. (4)), the magnetic fluxes can be obtained as functions of the armature position and the coil current (Eqs. (5-7).

$$\begin{bmatrix} \mathfrak{R}_e + \mathfrak{R}_l & 0 & \mathfrak{R}_l \\ 0 & \mathfrak{R}_e + \mathfrak{R}_r & -\mathfrak{R}_r \\ \mathfrak{R}_l & -\mathfrak{R}_r & \mathfrak{R}_l + \mathfrak{R}_r \end{bmatrix} \begin{bmatrix} \varphi_{ml} \\ \varphi_{mr} \\ \varphi_c \end{bmatrix} = \begin{bmatrix} \Phi_m \\ \Phi_m \\ Ni \end{bmatrix} \quad (4)$$

$$\varphi_{ml} = \frac{\mu A}{l_e} \left[\frac{1}{1+g/l_e-x^2/gl_e} \Phi_m + \dots \right. \\ \left. \dots - \frac{1+g/l_e-x/g-x^2/gl_e}{2(1+g/l_e-x^2/gl_e)} Ni \right] \quad (5)$$

$$\varphi_{mr} = \frac{\mu A}{l_e} \left[\frac{1}{1+g/l_e-x^2/gl_e} \Phi_m + \dots \right. \\ \left. \dots + \frac{1+g/l_e+x/g-x^2/gl_e}{2(1+g/l_e-x^2/gl_e)} Ni \right] \quad (6)$$

$$\varphi_c = \frac{\mu A}{l_e} \left[\frac{x/g}{1+g/l_e-x^2/gl_e} \Phi_m + \dots \right. \\ \left. \dots + \frac{2+l_e/g+g/l_e-x^2/gl_e}{2(1+g/l_e-x^2/gl_e)} Ni \right] \quad (7)$$

The force provided by the motor can be then obtained by applying the virtual work principle, by differentiating the system magnetic co-energy with respect to the armature position, Eq.(8-9).

$$F_m = \frac{\partial E_m}{\partial x} = \frac{\Phi_m}{2} \frac{\partial(\varphi_{ml} + \varphi_{mr})}{\partial x} + \frac{Ni}{2} \frac{\partial \varphi_c}{\partial x} \quad (8)$$

$$F_m = \frac{\mu A}{l_e g} \left[\frac{2\Phi_m^2 x/l_e}{(1+g/l_e-x^2/gl_e)^2} + \dots \right. \\ \left. \dots + \frac{\Phi_m Ni(1+g/l_e+x^2/gl_e)}{(1+g/l_e-x^2/gl_e)^2} + \frac{N^2 i^2(1+g/l_e)x/g}{2(1+g/l_e-x^2/gl_e)^2} \right] \quad (9)$$

As shown by Eq. (9), the magnetic force provided by the direct-drive motor is composed of three basic terms: the first one is exclusively due to the permanent magnets, it depends on the armature position and its effect can be viewed as a diminution of the centring spring stiffness; the second term is the most important force contribution, it is linear with the coil currents and it is produced by the interaction between the magnetic fluxes induced by the currents and the ones induced by the permanent magnets; the third term is exclusively due to the coils, and it tends to be important when the motor works with high currents [7].

2.3 Main requirements for application on aerospace servovalves

From the working principle point of view, there are no significant differences between a single-coil direct-drive motor and a quadruple-coil one, but specific design requirements must be addressed for the application on fault-tolerant aerospace servovalves:

- **Linearity:** a linear relationship between the command current and the valve displacement must be provided by the

motor in all the operating conditions. Nonlinear phenomena, such as magnetic saturation, magnetic hysteresis or sliding friction, must be kept at negligible levels, especially in the vicinity of the “null region” of the valve (centred motor armature);

- **Functionality in case of electrical failures:** the direct-drive motor must maintain its functionality even after two electrical failures, i.e. the working valve stroke must be completely covered also in the worst-case failure condition;
- **Functionality in case of contaminated fluid:** even in the worst-case failure condition¹, the motor must have sufficient force capability to shear a metallic chip blocked in one of the servovalve port (chip shear force). The cross-area of the blocked chip is generally referred to the maximum valve opening.

Undoubtedly, the coverage of each of the above-mentioned requirements must be assessed through experiments, but predictions and analyses are necessary during the whole design development, especially because the tests on the functionality in case of failures are complex and expensive. For these reasons, modelling and simulation activities become essential, and the need of accurate system models is evident.

3 Modelica model development

The model of the direct-drive motor has been divided into two sections: the one related to the permanent magnets, and the other to the quadruple coil.

3.1 Permanent magnet section

Previous works of the authors highlighted the role that the magnetic flux dispersion has in this type of system [6, 7]. For this reason, the permanent magnet section of the motor has been modelled with the magnetic circuit network shown in Fig. 3. The magnetic field of this motor section is composed of six fluxes: two ones linking the permanent magnets and the variable air gaps,

¹ Depending on the application, this aspect of the requirement could be relaxed, since extremely small probability of occurrence are related to multiple events.

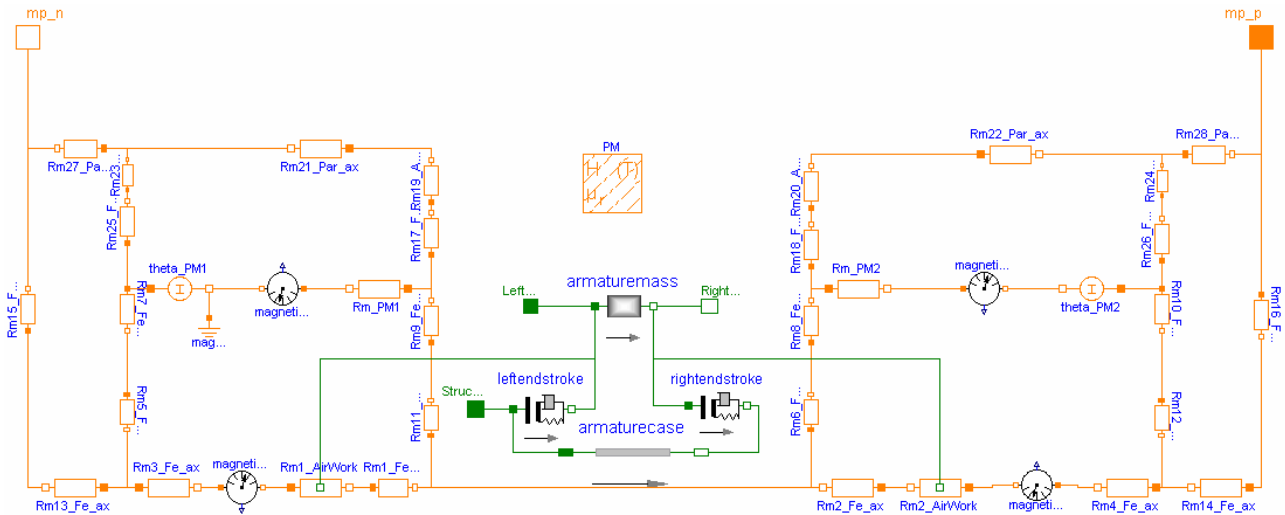


Figure 3 – Permanent magnet section of the motor model.

and four flux leakages that take into account the secondary paths of the magnetic fluxes.

The mechanical part of the model simply represents the armature mass and the containing case, with two *ElastoGap* components of the *Modelica.Mechanics.Translational* library, which simulate the left and right endstroke of the motor.

The interfaces of the resulting object-model are two magnetic ports for the integration with the magnetic network of the command coils, and two mechanical flanges, to be connected with the fixed structure of the hydraulic actuator and to the valve spool respectively.

3.2 Quadruple-coil section

The quadruple-coil section has been modelled taking into account of the secondary magnetic paths related to each coil (Fig. 4), so that the magnetic field contains four magnetic dispersion loops.

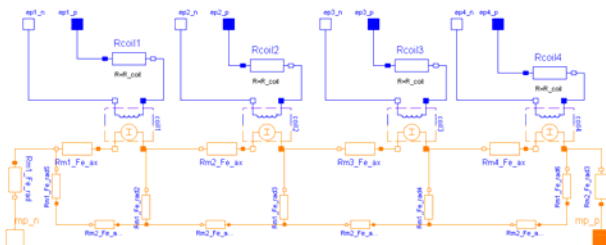


Figure 4 – Quadruple-coil section of the motor model.

The external interfaces of the resulting component are eight electrical pins (two ones for each of the four command electronics) and two magnetic

ports for the integration with the magnetic network of the permanent magnet section.

3.3 Complete model

The complete model of the direct-drive motor (Fig. 5) is finally obtained by magnetically linking the permanent magnets with the coils (reproducing the actual physical relationship between the two motor sections), and by adding a *Spring* and a *Stop* object-models coming from the *Modelica.Mechanics.Translational* library for simulating the centring spring and the effects of sliding friction respectively.

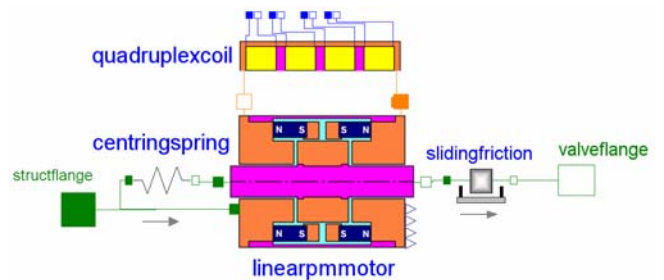


Figure 5 – Model of the fault-tolerant direct-drive motor.

3.4 Graphical user interface

The modelling activity led to the creation of three Modelica object-models: *linearpmmotor*, *quadruplexcoil* and *directdrivemotor*. All the object-models have been created providing the user with the possibility of tuning and selecting the system parameters via dialog box (e.g. geometrical dimensions, coil windings, coil

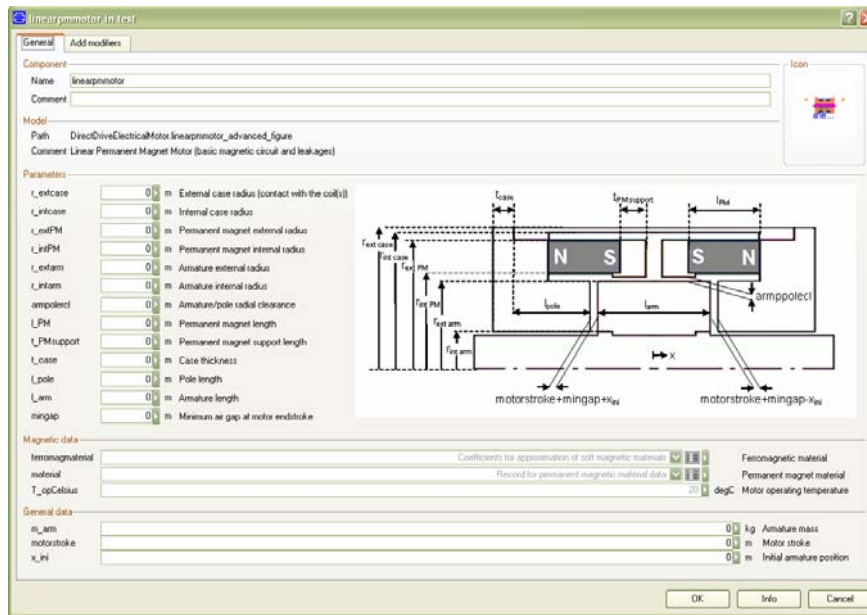


Figure 6 – Dialog box for the model of the permanent magnet section.

resistance, material properties, etc.).

An example is given in Fig. 6, where the graphical user interface of the *linearppmotor* object-model is reported.

4 Simulation and validation

The Modelica model of the motor has been developed with reference to the fault-tolerant direct-drive motor of the servovalve of a modern fly-by-wire actuator, which has been experimentally characterised by the authors during previous research activities [6]. The model validation has been achieved by comparing the Modelica results with the experimental data in terms of current-to-force and current-to-displacement curves, with reference to both the normal operating condition (four active coils) and the worst-case fault-tolerant condition (only two active coils).

In this section, the results of a Matlab-Simulink simulation of the motor [6] are also reported, in order to highlight the advantages of the object-oriented modelling with respect to a more classical approach.

4.1 Current-to-force characteristics

The current-to-force characteristics of the motor are reported in Fig. 7, where the net force (i.e. including the centring spring effect) is plotted as a function of the coil current for different armature

positions (centred and endstroke). The plot shown in Fig. 7.a is referred to the normal operating condition, while the Fig. 7.b refers to the case of only two active coils. The net force values have been normalized with respect to the required chip shear force of the valve.

The most interesting considerations can be done with reference to Fig. 7.a. The results show that both the Modelica (MDC) and the Simulink (SLK) models provide satisfactory results if a working condition with centred armature is concerned: both the direct-drive motor models exhibits a linear behaviour, with negligible errors with respect to experimental data. Furthermore, both the models provide good predictions in terms of cheap shear force capability². On the other hand, the MDC model is more accurate when the armature is placed at the endstroke and high positive currents are applied. This is because the magnetic saturation effects are not taken into account in the SLK model, and the magnetic force capability of the motor is overestimated.

The analytical model proposed in section 2.2, though simplified, can be useful for understanding the phenomena, since the magnetic saturation of soft ferrite parts is not taken into account as well. Equation 7 points out that the magnetic flux

² The chip shear force capability can be obtained from Fig. 6 by measuring the net force provided at endstroke (i.e. maximum cross-area of the blocked chip) when the maximum negative current is applied.

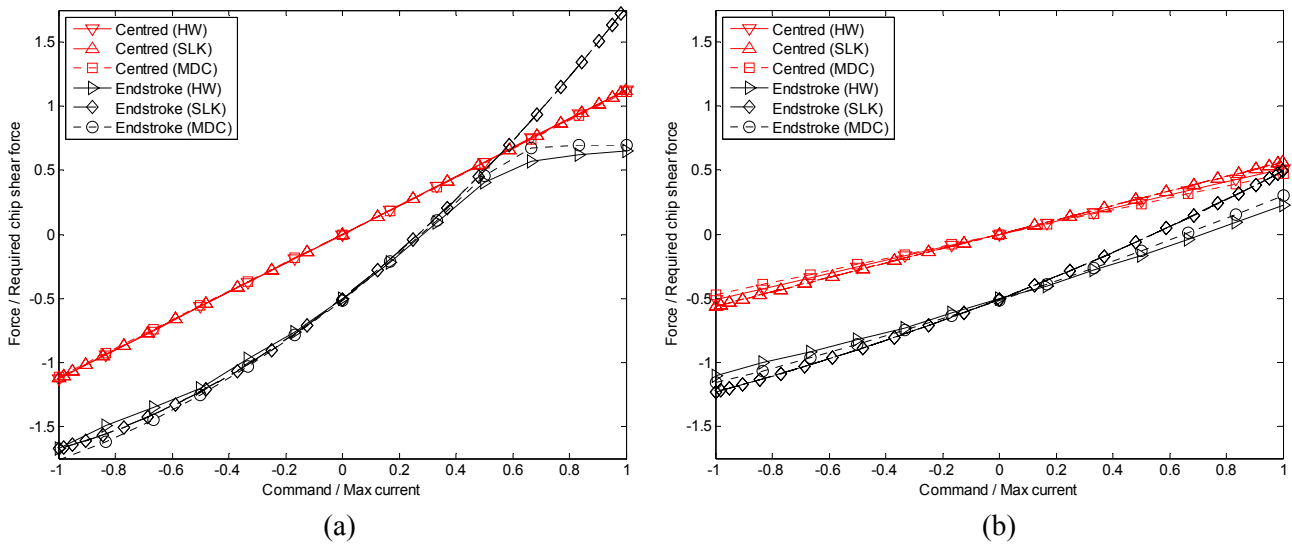


Figure 7 –Motor force characteristics with four active coils (a) and with two active coils (b).

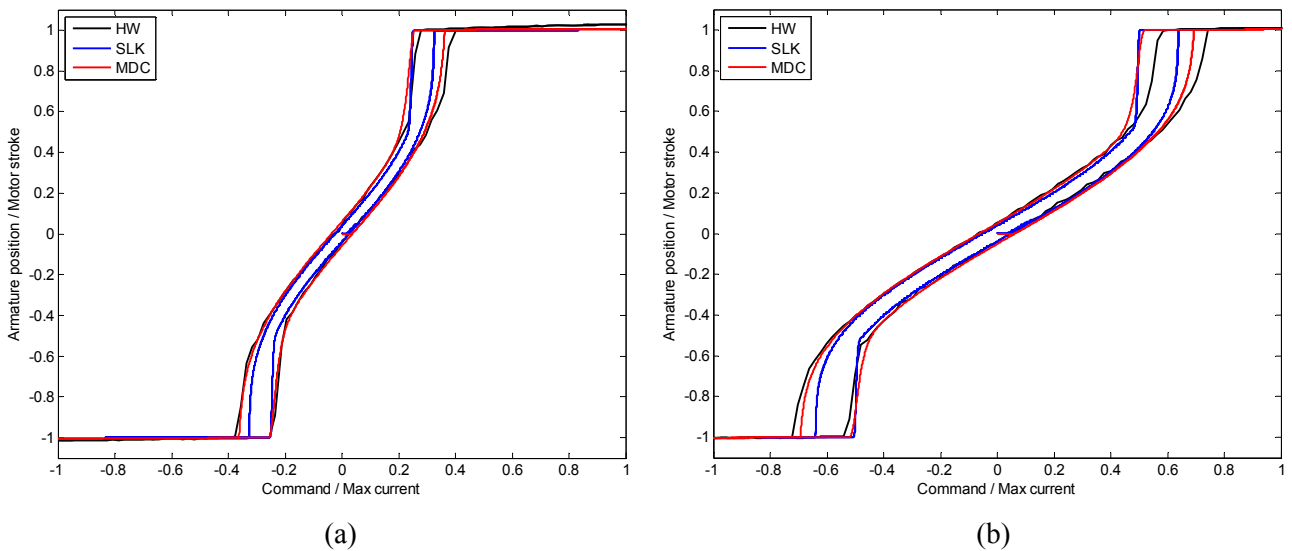


Figure 8 — Current-to-displacement curve with four active coils (a) and with two active coils (b).

linked to the coils at endstroke ($x=\pm g$) reaches very high values if the magnetomotive force related to the coils acts in the same direction of that of the permanent magnets (i.e. maximum positive current at $x=g$, and maximum negative current at $x=-g$), implying the possibility of magnetically saturating the soft ferrite parts. Without taking into account the magnetic saturation, the motor force at endstroke is parabolic with respect to coil current (Eq. (9)), and this behaviour is clearly exhibited by the SLK model (Fig. 7.a). On the other hand, the MDC model significantly deviates from the parabolic behaviour for currents higher than 0.4 A, satisfactorily reproducing the hardware response. This is because the MDC model inherently takes

into account the magnetic properties of the motor parts. Each reluctance of the magnetic network (Fig. 3) is defined as a physical object, characterised by specific geometrical and magnetic properties (material properties can be directly defined by the user or selected on a pre-defined database [5]).

Concerning Fig. 7.b, where the fault-tolerant working condition is concerned, the differences between the models demonstrate to be minor (magnetic saturation is not present, since the magnetomotive force of the coils is halved), even if the prediction errors are reduced with the MDC model.

4.2 Current-to-displacement characteristics

Figure 8 shows the comparison between the simulation and the experimental data in terms of current-to-displacement curves. The results are obtained by measuring the armature displacement while a sinusoidal low-frequency command current ($\pm i_{max}$ at 0.02Hz) is applied to the coils.

It can be noted that the both the models match very well the experimental data in both the operative conditions, even if the prediction errors tend to increase when the armature approaches the endstrokes.

4.3 Effects of the soft ferrite magnetic properties on motor performances

During the development of the motor models, no specific information about the properties of the soft ferrite parts was available. This aspect is not critical for the most applications, since electromagnetic actuators are designed to avoid magnetic saturation and the reluctances related to the soft ferrite parts are negligible with respect to air gaps or rare-earth magnets. As shown in the proposed study, this approach is not suitable for aerospace application, since the design is basically driven by low-weight, high-performance, safety-critical requirements, and system nonlinearities can become important.

Actually, the MDC results shown in Figs. 7-8 have been obtained after a specific sensitivity analysis carried out by varying the material of the soft ferrite parts of the motor. The activity has been initially performed by selecting the materials provided by the pre-defined database of the *Modelica_Magnetic* library (Vacofer S2, Permenorm 3601 K3, Hyperm0, Vacoflux50). The effect of magnetic properties demonstrated to be minor if the soft ferrite parts do not saturate, while significant discrepancies from experiments have been observed in the “saturation region” with all the selected materials. A specific study has thus been done to define an appropriate B-H curve of the soft ferrite parts of the motor for obtaining a good experimental matching.

The results of this activity are reported in Figs. 9-10. Figure 9 shows the “tuned” B-H curve compared with two materials of the *Modelica_Magnetic* database, while Fig. 10 reports the current-to-force curves at endstroke (four coils active) for hardware, SLK model and two MDC models, the one using the Vacoflux50 material and the other using the “tuned” material.

The model accuracy in the saturation region strongly depends on the transition to magnetic saturation, which is assumed to be more abrupt for the “tuned” material (Fig. 9).

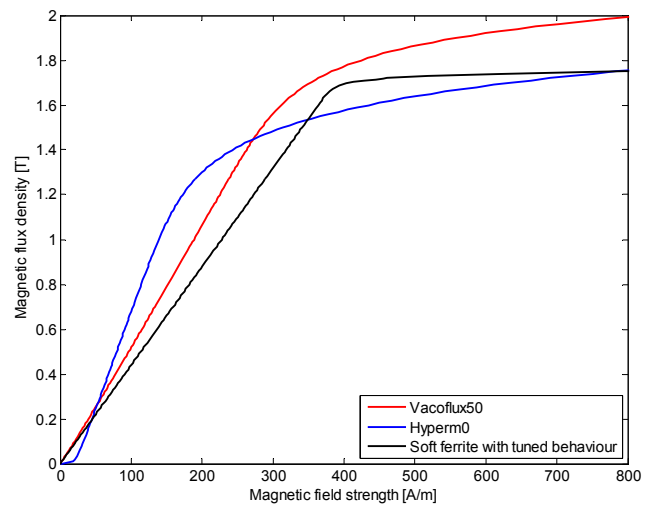


Figure 9 – B-H curves of tested soft ferrite material.

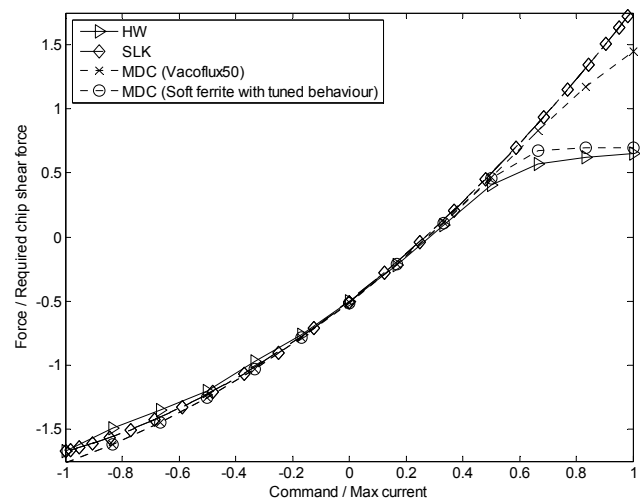


Figure 10 – Effects of soft magnetic material on motor force characteristics at endstroke (four active coils).

5 Conclusions

The Modelica model of a quadruple-coil direct-drive motor for aerospace servovalves is developed and validated with experimental data. The model predictions demonstrated to satisfactorily match the hardware response in normal operating condition (four active coils) as well as in the worst-case fault-tolerant condition (only two active coils). The inherent simulation of the magnetic saturation provided by the Modelica components allows to achieve accurate results in the whole range of operating conditions. The

results of the Modelica model are also compared with those provided by a Simulink model of the motor, pointing out the advantages of the object-oriented modelling for the study of complex electro-magnetic systems.

References

- [1] Pratt R. W., “Flight control systems: practical issues in design and implementation”, Institution of Engineering and Technology, Stevenage, 2000.
- [2] Miller F. G., “Direct drive control valves and their applications”, Proceedings of the IMechE International Conference on Aerospace Hydraulics and Systems, London (UK), 1993, pp. 1–16.
- [3] Elmqvist H., Mattsson S. E., and Otter M., “Modelica - the new object-oriented modeling language”, 12th European Simulation Multiconference (ESM'98), Manchester (UK), pp. 1-5, 1998.
- [4] Otter M., and Elmqvist H., “Modelica: language, libraries, tools, workshop and EU-project RealSim”, Simulation News Europe, pp. 3-8, 2000.
- [5] Bodrich T., Roschke T., “A magnetic library for Modelica”, Proceedings of the 4th International Modelica Conference, Hamburg (Germany), Vol. 2, pp. 559-565, 2005.
- [6] Di Rito G., and Galatolo R., “Experimental and theoretical study of the electrical failures in a fault-tolerant direct-drive servovalve for primary flight actuators”, Proceedings of the Institution of Mechanical Engineers, Part I, Journal of Systems and Control Engineering, v. 222, no. 18, 2008, pp. 757-769.
- [7] Di Rito G., “Experimental validation of theoretical and numerical models of a DDV linear force motor”, Proceedings of the 3rd FPNI-PhD Symposium, 2004, pp. 105–114.